diversity

MDPI

Article

Phylogeography and Genetic Structure of Sand Dune Specialist *Stilpnolepis centiflora* (Asteraceae) in Northwest China Revealed by Molecular Data

Xiaojun Shi [1,*], Xiaolong Jiang [2], Hongxiang Zhang [3] and Juan Qiu [1]

[1] College of Life Sciences, Xinjiang Agricultural University, Urumqi 830052, China; xjqiujuan@163.com
[2] The Laboratory of Forestry Genetics, Central South University of Forestry and Technology, Changsha 410004, China; xiaolongjiang1@gmail.com
[3] State Key Laboratory of Desert and Oasis Ecology, Xinjiang Institute of Ecology and Geography, Chinese Academy of Sciences, Urumqi 830011, China; zhanghx561@ms.xjb.ac.cn
* Correspondence: shixj@xjau.edu.cn

Abstract: *Stilpnolepis centiflora* is an endemic annual herb in the Asteraceae family found across five sand deserts in Northwest China. We aimed to investigate the genetic structure of *S. centiflora* and attempt to link species evolution with desert formation during the Pleistocene era. We used sequence data from nuclear and chloroplast genes to investigate genetic diversity among 28 populations. We analyzed sequence data using network analysis, spatial analysis of molecular variance (SAMOVA), and a Mantel test. We then used a molecular clock to place the genetic patterns in a temporal framework and tested for signals of expansion using neutrality tests and by determining mismatch distributions. Six distinct haplotypes and 31 ribotypes were identified. Significant chloroplast DNA population subdivision was detected (G_{ST} = 0.952; N_{ST} = 0.976), but only moderate nrDNA subdivision (G_{ST} = 0.360; N_{ST} = 0.579) was detected. SAMOVA revealed four diverging groups of related haplotypes, coinciding with the boundaries of deserts. Molecular dating suggests that the clades representing different deserts diverged from 1.2 to 0.20 Ma, concordant with the Kun-Huang Movement of Qinghai Tibet Plateau uplift and a glacial event (Naynayxungla) during the Middle–Late Pleistocene. The disjunction of *S. centiflora* among different deserts was correspondingly reflected in the examined genetic traits with consistent spatiotemporal evolution between species and deserts. Therefore, the evolutionary dynamics of *S. centiflora* appear to have been driven by geological movement and climate change. The patterns described here are potentially useful to conservation biologists and may serve as a model for other sand-obligate organisms found in the deserts of Northwest China.

Keywords: chloroplast DNA; ITS; *Stilpnolepis*; allopatric divergence; genetic structure

Citation: Shi, X.; Jiang, X.; Zhang, H.; Qiu, J. Phylogeography and Genetic Structure of Sand Dune Specialist *Stilpnolepis centiflora* (Asteraceae) in Northwest China Revealed by Molecular Data. *Diversity* **2022**, *14*, 104. https://doi.org/10.3390/d14020104

Academic Editor: Michael Wink

Received: 22 November 2021
Accepted: 29 January 2022
Published: 31 January 2022

1. Introduction

Historically, geographic and climatic events have had a strong influence on the genetic diversity of species [1]. In the Northern Hemisphere, most biogeographical studies on plants have shown that those currently inhabiting formerly glaciated areas retreated to the southern glacial refugia, and then expanded to their modern ranges after the last glacial maximum (LGM) [2–4]. However, the impact of these climatic oscillations was different on different continents. In the desert regions of Northwest China, lacking continental glaciers, glacial periods had the primary effect of intensifying aridity. How did desert plants respond to these conditions? Since desert plants tolerate arid conditions, the climatic oscillations might have affected their survival less [5,6]. On the other hand, the mobilization and accumulation of sand were greatly enhanced. Thus, the distribution of desert plants might have increased or diminished during climatic oscillations because of the expansion

or shrinkage of desert sand dunes [7,8]. In addition, deserts served as geographical barriers and thus could have promoted species differentiation in desert organisms [9–13].

Large sand deserts extend from northwestern to northern China, including the great Taklimakan Desert and the five deserts considered in this study. These deserts may have played an important role in the speciation and evolution of plants in the arid regions of Northwest China [14]. Desert formations resulted from the effects of an intensely arid climate on Quaternary paleo-eolian sands [15–17], presumably related to the uplift of the Tibetan Plateau [18–20] during the period when large-scale sand dunes expanded [21–23].

Phylogeographical analyses can trace the influence of paleoenvironments and climate change on species distribution and population demography [24]. Previous phylogeographical studies conducted in the arid regions of Northwest China provide an understanding of the spatiotemporal diversification patterns associated with environmental and climatic change; examples include *Gymnocarpos przewalskii* [25], *Reaumuria soongarica* [7], *Nitraria sphaerocarpa* [8], and *Juniperus sabina* [14]. These studies demonstrated that climate oscillations have profound effects on the evolutionary processes of native desert species, resulting in allopatric divergences [14], regional range expansion [7], and the contraction or fragmentation of population distribution [8]. However, little is known about how desert species in Northwest China responded to past geological changes, especially during the formation and development of deserts. In addition, most studies have focused on shrub species instead of herbs, which are better suited for depicting some aspects of plant evolution due to their short life cycle.

The annual herb *Stilpnolepis centiflora* belongs to Anthemideae Cass. (Asteraceae) [26]. *Stilpnolepis* is considered a monospecific genus based on research about its life history, geographical distribution, and pollen morphology [27,28]. *S. centiflora* is an endemic species with disjunct distribution between five deserts (Figure S1) [27], primarily found on mobile sand dunes and flat sand sheets between dunes. Its flowers are pollinated by a wide variety of insects such as bees and flies, and the seeds are usually dispersed by gravity. Due to the uplift of the QTP and climate change during the Quaternary period, the geographical and natural environments varied dramatically in the arid land region in Northwest China, especially in desert regions. *S. centiflora*, as an endemic desert plant species, has historically experienced many environmental and geographic changes; hence, we hypothesized that the present distribution of *S. centiflora* is the consequence of a series of geomorphological adjustments in the region.

In the present study, we amplified and sequenced two maternally inherited chloroplast DNA (cpDNA) markers (psbA-trnH, trnQ-rps16) as well as the biparentally inherited internal transcribed spacer (nrITS) region. The data were combined to detect intraspecific divergence and possible hybridization and introgression events [29,30]. Our objective for the present study was to understand the level of genetic variation, population structure, and genetic divergence of S. centiflora using cpDNA and ITS markers.

2. Materials and Methods

2.1. Sampling Methods

Two hundred eighty *S. centiflora* individuals were collected from 28 populations distributed across five deserts, covering most areas where the species is found distributed in China. The sample consisted of four populations (populations 1–4) from the Kubuqi Desert, four populations (populations 5–8) from the Mu Su Desert, four populations (populations 9–12) from the Badain Jaran Desert, eight populations (populations 13–20) from the Ulan Buh Desert, and eight populations (populations 21–28) from the Tengger Desert (Table S1). In each population, whole fresh plant organs with flowers/fruits were collected as voucher specimens, and young leaf samples were collected from 10 individuals and dried in silica gel. When sampling, a distance of at least 30 m was maintained between individuals within the same population to increase the likelihood of sampling interindividual variation. We used three species as external groups (*Elachanthemum intricatum*, *Artemisia montana*, and *Artemisia frigida*). *Elachanthemum intricatum* was sampled and used as an

outgroup in the subsequent analyses. The target sequences of the other two outgroup species were extracted from the chloroplast genome sequence downloaded from GenBank: *Artemisia montana* (KF887960.1) and *Artemisia frigida* (JX293720.1). Voucher specimens were collected and deposited in the Herbarium of Xinjiang Institute of Ecology and Geography, Chinese Academy of Science (XJBI).

2.2. Laboratory Procedures

DNA was extracted using a modified CTAB protocol [31]. Firstly, we amplified the two chloroplast (cpDNA) genes *psb*A-*trn*H and *trn*Q-*rps*16 intergenic spacers using primers and cycling conditions described by Shaw et al. [32,33]. We used a total of 30 cycles of denaturation at 94 °C for 30 s, annealing at 52 °C for 30 s, and elongation at 72 °C for 90 s, and a final elongation at 72 °C for 10 min. Secondly, we amplified the nuclear internal transcribed spacer (ITS) in 250 individuals, using forward (ITS1) and reverse primer (ITS4) for amplification for both internal transcribed spacers and the 5.8S gene [34]. Amplification products were purified from 1.5% low-melting agarose gels, and the desired PCR fragment was recovered with a UNIQ-10 kit (Shanghai SBS, Biotech Ltd., Shanghai, China) according to the manufacturer's recommendations. Sequencing reactions were conducted on the recovered PCR fragment using the forward or reverse primers of the amplification reactions and the DYEnamic ET Terminator Kit (Amersham Pharmacia Biotech, Cambridge, UK), followed by sequencing with an Applied Biosystems 3730 Capillary DNA DNA Analyzer (Shanghai Sangon Biological Engineering Technology & Services Co., Ltd., Shanghai, China). DNA sequences were edited using SeqMan (Lasergene, DNASTAR Inc., Madison, WI, USA) and initially aligned with Clustal X 1.81 [35].

2.3. CpDNA and ITS Sequence Analysis

For cpDNA, we concatenated the two chloroplast gene fragments used in the analysis. For ITS, haplotypes of heterozygous individuals were reconstructed with the PHASE algorithm implemented in DnaSP 5.10 [36], using a recombination model with no assumption about rate variation and an initial estimate of 0.0004. The Markov chain Monte Carlo (MCMC) method was run for 1000 iterations with a burn-in of 100, a thinning interval of 1, and an output probability threshold of 0.9. This method is a reliable way to infer differences in alleles in heterozygotes and, therefore, a suitable alternative to cloning and omitting unresolved genotypes for phylogeographical analysis [37]. Identical haplotypes for cpDNA and phased nrDNA alleles were collapsed using DNASP 5.10. Newly identified sequences were submitted to GenBank under the accession numbers MF416962-MF417003 (Tables S2 and S3).

Phylogenetic trees were constructed using the neighbor-joining (NJ) method implemented in MEGA version 11.0 [38]. The NJ analysis incorporated Kimura's 2-parameter model of DNA evolution [39]. The relationships between cpDNA haplotypes and ribotypes for ITS were estimated with Network version 4.6.0.0 using the median-joining method [40,41].

Nucleotide diversity (π), haplotype diversity (H), and the number of segregating sites (S) were calculated from both cpDNA and ITS data using Arlequin 3.5 [42]. Isolation-by-distance analysis was conducted using a Mantel test implemented in Alleles in Space (AIS) [43]. Mantel's test explicitly tests the plausibility of an isolation-by-distance scenario in AIS to analyze the relationships between genetic and geographic distances between sampling localities.

Genetic differentiation among populations was evaluated using the G_{ST} and N_{ST} coefficients implemented in Permut CpSSR v.2.0 [44] based on 2000 random permutations of haplotypes across populations. If N_{ST} is significantly higher than G_{ST}, then genealogically closely related haplotypes tend to occur together within populations, providing evidence for phylogeographical structure.

We used spatial analysis of molecular variance (SAMOVA 2.0) to partition the populations into genetically and geographically homogeneous groups [45]. Data from cpDNA

and nrDNA were separately analyzed using 100 simulated annealing processes by varying K (number of groups) from 2 to 10. The best K value was selected according to when F_{CT} reached a plateau. In addition, we performed Bayesian analysis of population structure as implemented in Structure version 2.2 to infer the most likely number of population genetic clusters (K) in the cpDNA dataset [46]. K ranged from 1 to 10, with 10 replicates performed for each K using a burn-in period of 2×10^5 and MCMC of 5×10^4. For this analysis, a "no-admixture model" and independent allele frequencies were chosen. The most likely K value was determined based on the Delta K statistic according to Pritchard et al. [47] using Structure Harvester [48]. To investigate the level of genetic variation among and within groups, hierarchical analysis of molecular variance (AMOVA) was performed using multiple categorical variables (populations, haplotypes, sampling locations, clade, and lineage) [49]. AMOVA was conducted using Arlequin v.3.5 and 1000 random permutations.

Bayesian Evolutionary Analysis Sampling Trees (BEAST) v.1.8.2 [50] was used to reconstruct haplotype gene trees and simultaneously estimate the divergence times between haplotypes. We used a constant-size coalescent tree prior and GTR substitution model in the analysis. As there is no fossil record of *Stilpnolepis*, we adopted a substitution rate method. The cpDNA substitution rates of most angiosperm species were estimated to vary between 1 and 3×10^{-9} substitutions per site per year (s/s/y). Due to the uncertainty of the rates, we used normal distribution priors with a mean of 2×10^{-9} and an SD of 6.080×10^{-10} within the 95% distribution range to estimate divergence times [51]. Although molecular clock estimates vary and, in most cases, only provide crude estimates of divergence times, they can provide insight into the approximate timing of divergences. Hence, we interpreted our molecular clock findings with an appropriate level of caution. The posterior distributions of the parameters in the MCMC analyses were approximated with 10 million steps in each analysis and sampled every 1000 generations. Convergence of the parameters sampled was checked with the program Tracer v.1.5 to examine the highest effective sampling size values (ESSs > 200) for all parameters [52]; the burn-in steps were discarded to estimate the posterior probability distribution of divergence time at the relevant node. FigTree 1.3.1 [53] was used to display the sampled trees.

The demographic history of the predicted groups based on phylogenetic analysis of haplotypes was assessed for all 28 populations; only 4 populations from Badain Jaran Desert and 8 populations from Tengger Desert used three methods implemented in Arlequin v. 3.5. Firstly, Tajima's D [54] and Fu's Fs statistics [55] were used to explore evidence for demographical expansions using a null distribution of 10,000 coalescent simulations. Significantly negative values indicate that population expansion has occurred. Secondly, mismatch distributions [56] were calculated to test for signals of demographic expansion with populations undergoing exponential growth expected to show a smooth unimodal mismatch distribution curve [57]. The significance of sum of squared deviations (SSD) and raggedness indices was determined by bootstrap resampling (10,000 replicates). Similarly, the HRag significance was determined for SSD with 1000 parametric bootstrap replicates. When an expansion model could not be rejected, we estimated the expansion time (t) as $t = \tau/2u$, where τ is calculated as the time to expansion in mutational units and u is the mutation rate per generation for the whole sequence. The u is equal to μgk, where μ is the substitution rate in substitutions per site per year (s/s/y) and k is the two-cp sequence length. The generation time (g) was estimated to be one year. The substitution rate range of the two combined cpDNA-IGS regions was perceived as the minimum and maximum mutation rates of 1.0×10^{-9} s/s/y and 3.0×10^{-9} s/s/y [58].

3. Results

3.1. Genetic Variation Based on Plastid Sequence

The total alignment length of the two chloroplast regions (*psb*A-*trn*H, *trn*Q-*rps*16) surveyed across 280 individuals from 28 populations of *S. centiflora* was 1345 bp, including nine substitutions that were represented by six haplotypes (H1–H6) (Table S4). The haplotype compositions for each population are presented in Table 1. Although the cpDNA data

revealed high haplotype diversity (h = 0.794) across all 28 populations, only populations 9 and 10 sampled from Badain Jaran Desert had two haplotypes each (H5 and H6) with a haplotype diversity of 0.36 and 0.20, respectively. Nucleotide diversity was computed across all populations, and populations 9 and 10 were significantly low, varying from 0.0003 to 0.002. The remaining 26 populations only had a single haplotype with a haplotype and nucleotide diversity of zero. Three of the six haplotypes (H1, H4 and H5) were shared between two or three of the five deserts. H1 was shared in two of the populations sampled from Ulan Buh Desert and four of the populations from Tengger Desert, whereas H4 was shared among five of the populations from Ulan Buh Desert and one population from Tengger Desert. H5 was common among the five populations sampled from Badain Jaran Desert, one population from Ulan Buh Desert, and three populations from Tengger Desert. H2 and H3 were specific to Kubuqi Desert and Mu Us Desert, respectively, whereas H5 and H6 were observed together in two of the populations collected from Badain Jaran Desert (Table 1; Figure 1). The within-population gene diversity (H_S) was significantly lower (0.020) than total gene diversity (H_T) (0.820, Table 2).

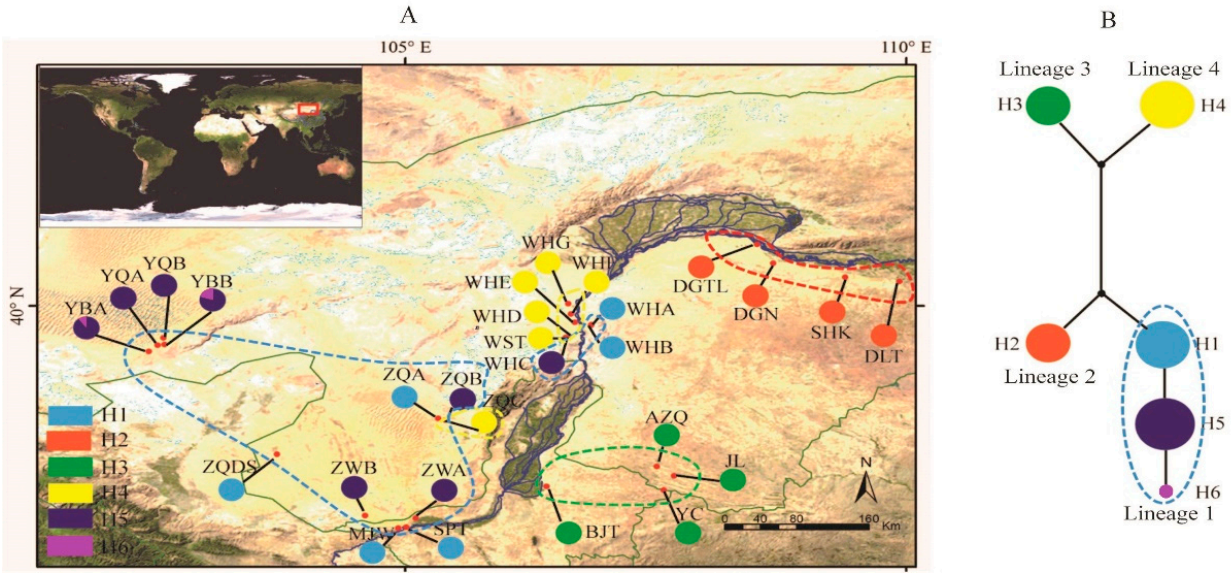

Figure 1. (**A**) Geographic distribution of cpDNA haplotypes (H1–H6) detected in the 28 populations of *Stilpnolepis centiflora*. The colored dashed curve lines delimitate the population groups (I–IV) resulting from SAMOVA and network analysis. Blue: lineage I; red: lineage II; green: lineage III; yellow: lineage IV. (**B**) The size of circles corresponds to the frequency of each haplotype. The small black circles on the branches represent hypothetical missing haplotypes.

The total gene diversity H_T (0.820) was significantly higher than the average within-population diversity H_S (0.020); therefore, both G_{ST} (0.976) and N_{ST} (0.986) were high (Table 2). Around 92.9% of the variation was attributed to genetic differentiation among the five desert regions; between-population variation accounted for just over three-quarters (98.6%) of the total variation, indicating strong differentiation and less gene flow between regions and populations (Table 3). Within each of the five regions, between-population differentiation was similarly low (Table 3). Overall, these results strongly indicate that haplotypes are geographically structured across the distribution range of the species.

Table 1. Summary of the 28 *Stilpnolepis centiflora* populations' sampling information and genetic diversity based on chloroplast DNA (cpDNA) and internal transcribed spacer (ITS) data. See Table S4 for details of the different haplotypes and ribotypes.

Code/Location	Latitude/Longitude (N/E)	cpDNA				ITS			
		N	Haplotype	h	π	N	Ribotypes	h	π
Total		280		0.7944	0.0020	250		0.8140	0.0030
Kubuqi Desert									
1 SHK	39.64°/106.60°	10	H2	0	0	22	R1, R2, R3, R4	0.6623	0.0028
2 DGN	40.71°/108.51°	10	H2	0	0	20	R1, R2, R5, R6, R7	0.6632	0.0034
3 DGTL	40.49°/108.67°	10	H2	0	0	18	R1, R2, R5, R6, R8	0.7451	0.0026
4 DLT	40.28°/109.93°	10	H2	0	0	18	R1, R2, R8	0.5817	0.0026
Mu Us Desert									
5 AZQ	40.33°/109.39°	10	H3	0	0	16	R2, R8, R9, R10, R13	0.8250	0.0020
6 BJT	38.05°/107.68°	10	H3	0	0	12	R6, R14,	0.3030	0.0025
7 YC	37.93°/106.41°	10	H3	0	0	14	R1, R8, R10	0.4835	0.0021
8 JL	37.46°/105.01°	10	H3	0	0	20	R1, R8, R9, R10, R11, R12, R13	0.6895	0.0025
Badain Jaran Desert									
9 YBA	39.35°/102.34°	10	H5 H6	0.3556	0.0005	12	R5, R6, R7, R17	0.7143	0.0012
10 YBB	39.55°/102.53°	10	H5 H6	0.2000	0.0003	14	R6, R7, R17	0.4394	0.0007
11 YQA	39.56°/102.60°	10	H5	0	0	24	R5, R6, R7, R17	0.4312	0.0007
12 YQB	39.64°/102.58°	10	H5	0	0	24	R5, R6, R7, R17, R31	0.7391	0.0014
Ulan Buh Desert									
13 WHA	39.78°/106.86°	10	H1	0	0	14	R5, R6, R15, R17	0.6923	0.0012
14 WHB	39.78°/106.85°	10	H1	0	0	20	R5, R6, R15, R17	0.6105	0.0010
15 WHC	39.64°/106.63°	10	H5	0	0	20	R5, R6, R7, R15, R24	0.6263	0.0013
16 WHD	39.64°/106.6°	10	H4	0	0	20	R5, R6, R7, R17, R24	0.4421	0.0008
17 WHE	39.91°/106.66°	10	H4	0	0	16	R6, R7, R24	0.6583	0.0016
18 WHF	39.82°/106.69°	10	H4	0	0	16	R6, R17	0.5000	0.0007
19 WHG	40.03°/106.63°	10	H4	0	0	16	R6, R17	0.1250	0.0002
20 WST	38.16°/107.51°	10	H4	0	0	12	R6, R15, R16, R17	0.5606	0.0009
Tengger Desert									
21 ZQA	38.71°/105.33°	10	H1	0	0	22	R5, R6, R7, R17, R29, R30	0.7619	0.0015
22 ZQB	38.69°/105.40°	10	H5	0	0	20	R5, R6, R7, R17, R23, R27, R28	0.6895	0.0017
23 ZWA	37.57°/105.10°	10	H5	0	0	16	R6, R7, R17, R23, R24	0.7667	0.0017
24 ZWB	37.59°/104.6°	10	H5	0	0	20	R6, R7, R17, R25	0.7105	0.00140
25 ZQC	38.55°/105.35°	10	H4	0	0	10	R6, R7, R17, R26	0.7333	0.0013
26 MJW	37.89°/107.58°	10	H1	0	0	12	R7, R17	0.5455	0.0015
27 SPT	37.45°/104.93°	10	H1	0	0	28	R6, R7, R17, R18, R19, R20, R21	0.8042	0.0018
28 ZQDS	38.30°/103.72°	10	H1	0	0	22	R5, R6, R7, R17, R22	0.7792	0.0015

N, h and π refer to number of individuals, haplotype diversity, and nucleotide diversity within populations, respectively.

Table 2. Estimation of gene diversity (H_S, H_T) and gene differentiation (G_{ST}, N_{ST}) across all populations of *Stilpnolepis centiflora*.

Date	H_S	H_T	G_{ST}	N_{ST}
cpDNA	0.020 (0.014)	0.820 (0.018)	0.976 (0.018)	0.986 (0.010)
ITS	0.617 (0.031)	0.817 (0.037)	0.244 (0.042)	0.485 (0.053)

H_S, average gene diversity within populations; H_T, total gene diversity; G_{ST}, interpopulation differentiation; N_{ST}, number of substitution types. Values are means (± SE in parentheses).

Table 3. Hierarchical analysis of molecular variance (AMOVA) based on chloroplast DNA (cpDNA) and internal transcribed spacer (ITS) data of 280 individuals from 28 *Stilpnolepis centiflora* populations.

Source of Variation	cpDNA			ITS		
	d.f.	PV (%)	Fixation Index	*d.f.*	PV (%)	Fixation Index
Among populations	27	98.6	F_{ST} = 0.986	27	46.68	F_{ST} = 0.467
Within populations	252	1.4		470	53.32	
Total	279			497		
Five deserts						
Among deserts	4	92.9	F_{SC} = 0.841 **	4	35.17	F_{SC} = 0.240 **
Among populations within deserts	23	5.97	F_{ST} = 0.989 **	23	15.58	F_{ST} = 0.508 **
Within populations	252	1.13	F_{CT} = 0.929 **	470	49.25	F_{CT} = 0.352 **
Total	279			497		
Four lineages						
Among lineages	3	91.73	F_{SC} = 0.879 **			
Among populations within lineages	24	7.27	F_{ST} = 0.990 **			
Within populations	252	1	F_{CT} = 0.917 **			
Total	279					

d.f., degrees of freedom; F_{ST}, correlation within populations relative to the total; PV, percentage of variation; SS, sum of squares; VC, variance components. **, $p < 0.01$; 1000 permutations.

The spatial genetic structure analysis based on cpDNA using SAMOVA showed a sharp increase in F_{CT} values from K = 2 to K = 10 and then reached a plateau at K > 7 (Figure S2), which suggests four possible groups. The groups obtained using Structure revealed the substantial phylogeographic patterns and additionally allowed recovering information about the hierarchical relationships among the groups of populations. When K = 2, individuals from the TGL-BDJL group were separated from other populations. When K = 4, further substructuring was observed that corresponds to the TGL-BDJL, WLBH, MWS, and KBQ geographic groups (Figure S3). A subsequent analysis was conducted to corroborate the structures detected with this first analysis, excluding TGL-BDJL population groups from the dataset to determine if any additional substructure could be detected. In the second analysis, the highest peak at K = 3 corresponded to MWS, WLBH, and KBQ geographic groups, which confirmed the genetic substructure detected by the SAMOVA and network analysis (Figures S2 and S3). The topology of the corresponding grouping configuration resembled that obtained from the NJ analyses (Figure 2). As shown in Figures 1A,B and 2, the four groups (a–d) were almost completely allopatric and corresponded to different desert regions (a: Badain Jaran Desert–Tengger Desert; b: Kubuqi Desert; c: Mu Us Desert; d: Ulan Buh Desert).

Three levels of hierarchical AMOVA (Table 3) conducted on cpDNA revealed significant great genetic differentiation among the groups (F_{ST} = 0.990, $p < 0.001$). Overall, these results strongly indicate that haplotypes are geographically structured across the distribution range of the species. Mantel test showed a moderate but significant correlation (r = 0.304, $p < 0.05$) between genetic differentiation and geographic distance among populations (Figure S4).

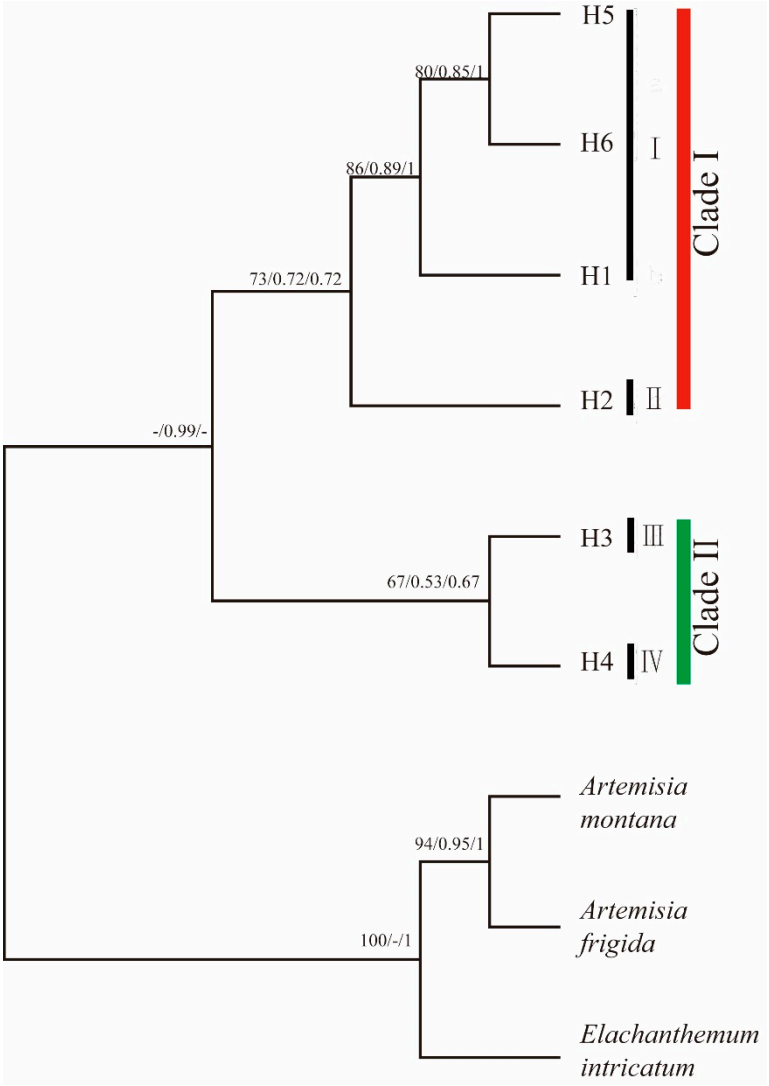

Figure 2. Phylogenetic relationships of the identified haplotypes of *Stilpnolepis centiflora* using *Elachanthemum intricatum*, *Artemisia montana*, and *Artemisia frigida* as outgroups by neighbor-joining method. Neighbor-joining bootstrap values are shown above branches.

3.2. Genetic Variation, Ribotype Distribution, Population Structure, and Phylogenetic Relationships between Ribotypes Based on ITS Sequence

Ribotype reconstruction of ITS sequences in PHASE resulted in highly supported ribotype pairs ($p > 0.90$) for 250 individuals (500 sequences in total). Although the ITS commonly represents a family of genes, sequences did not show extremely high levels of polymorphism, and manual alignment was straightforward. The aligned ITS data set (714 bp) yielded 31 ribotypes from the 500 sequences (Table S5). Among the 31 determined ribotypes, 7 nuclear ribotypes (R1, R2, R5, R6, R7, R8, R17) were relatively common (Figure 3). R6 was widely distributed in the five deserts; R5 and R7 were shared in WLBH, TGL, BDJL, and KBQ; R17 was shared in TGL, WLBH, and BDJL; R1, R6, and R8 were shared in KBQ and MWS. R24 was shared in WLBH and TGL. Of the 23 rare remaining ribotypes, 6 were restricted to MWS (R9, R10, R11, R12, R13, R14), 12 were restricted to TGL (R18, R19, R20, R21, R22, R23, R25, R26, R27, R28, R29, R30), 2 were restricted to KBQ (R3 and R4), 2 were restricted to WLBH (R15 and R16), and 1 was restricted to BDJL (R31) (Table 1). Ribotype diversity computed within populations varied from 0.125 in the WHG population to 0.825 in the AZQ population with an overall mean value of 0.814 across the 28 populations. Nucleotide diversity within populations varied from 0.0002 in the WHG population to 0.0034 in the DGN population with an overall mean value of 0.003 across

the 28 populations (Table 1). Within-population gene diversity (0.617) was lower than total gene diversity (0.817) (Table 2).

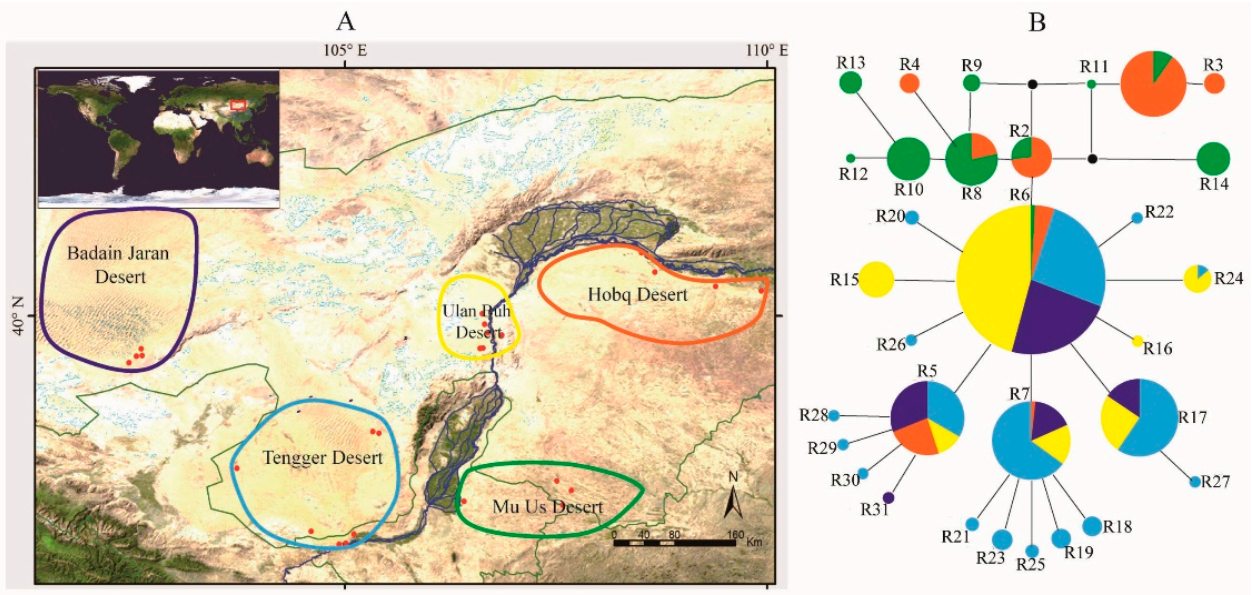

Figure 3. (**A**) The geographic distribution of the 28 *Stilpnolepis centiflora* populations in the deserts of northwestern China. Each desert is marked using different colors. (**B**) The networks of 31 ribotypes of *S. centiflora*. The size of circles corresponds to the frequency of each ribotype. Small black circles on the branches represent hypothetical missing ribotypes. Ribotypes are color-coded based on deserts: Purple: Badain Jaran; blue: Tengger; yellow: Ulan Buh; orange: Kubuqi; green: Mu Us.

For the ITS data, the phylogenetic relationships were reconstructed using NJ methods. Most of the 31 ribotypes did not form a well-supported clade (Figure S5), and the ribotype network (Figure 3B) contained the same relationships as the phylogenetic trees (Figure S5). The genealogical analysis of nuclear haplotypes (Figure 3B) showed that haplotype R6 differed from the others by one to five mutation steps. According to the ribotype network, there was no apparent association of ribotypes with geography. Compared with cpDNA data, *S. centiflora* showed lower population differentiation, with G_{ST} values of 0.244 for ITS data. The SAMOVA analysis of the ITS data did not show strong geographic patterning compared with analyses of the cpDNA sequences. Nonetheless, AMOVA revealed that differences among the four cpDNA groups (a–d identified) accounted for 39.68% of the total nrDNA variation compared with 14.14% among populations and 48.18% within populations (Table 3). The Mantel test based on ITS data revealed a significant isolation-by-distance pattern ($r = 0.2876$, $p < 0.001$) (Figure S4).

3.3. Demographic History

The neutrality tests did not support the occurrence of population expansions for all populations, Clade I, and Clade II (Figure 2). The mismatch distribution consisted of a double-peak curve (Figure 4A–C), which suggests that all populations, Clade I, and Clade II did not experience demographic expansion. The nonsignificant SSD statistics, HRag value, neutrality test, and multimodal mismatch distribution (Table 4) all suggest the *S. centiflora* population sizes remained relatively stable for long periods in the past (Figure 4; Table 4). However, the single-peak curve (Figure 4D) in the mismatch distribution for Lineage I is indicative of demographic expansion. Based on the corresponding τ values, assuming a substitution rate of between 1.0×10^{-9} and 3.0×10^{-9} s/s/y (see above), we estimated the possible expansion of *S. centiflora* in the Tengger–Badain Jaran Desert regions may have occurred between 0.08 and 0.26 Ma. The mismatch analysis and neutrality test were not conducted for Lineages I, II, and III since they each comprised only one haplotype.

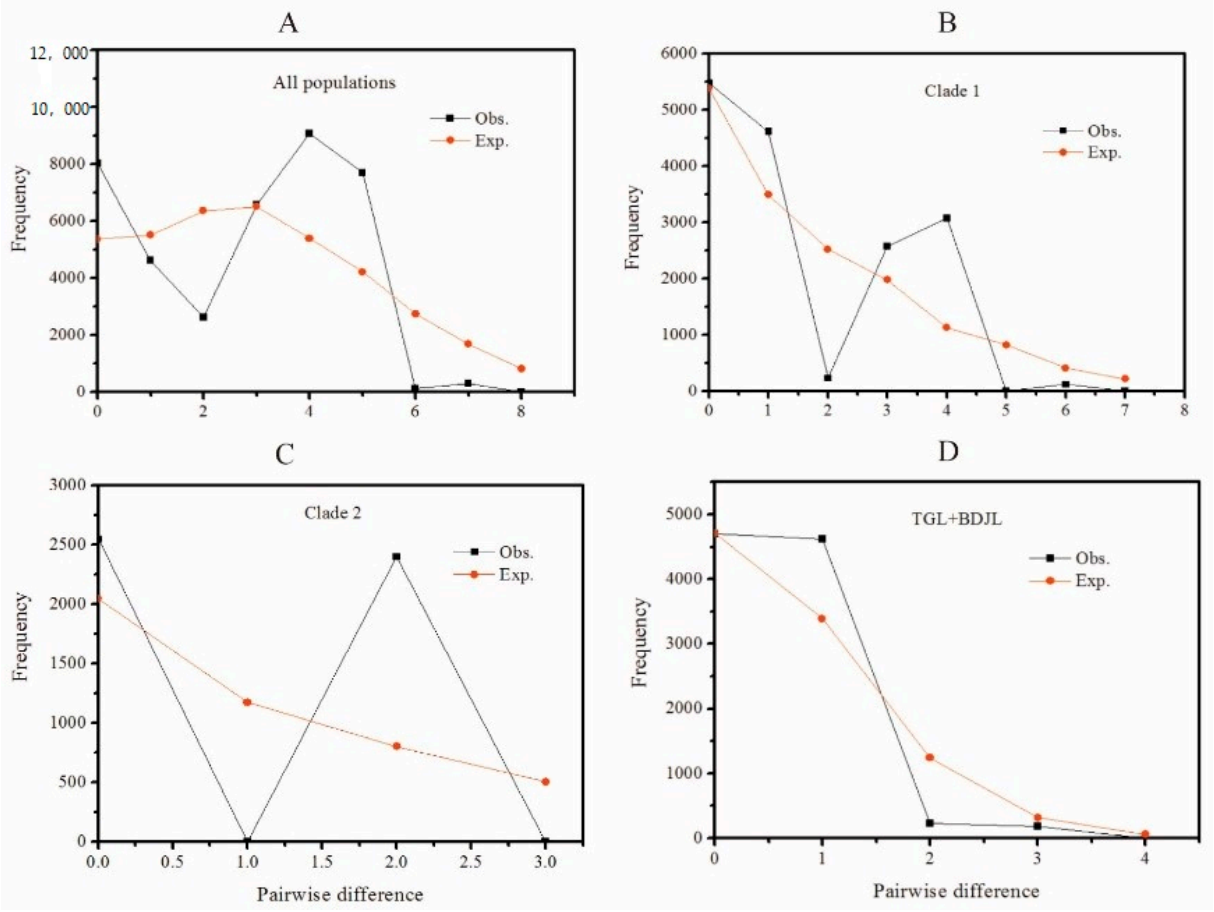

Figure 4. Mismatch distribution analysis for cpDNA data for all 28 populations (**A**), Clade 1 (**B**), Clade 2 (**C**), and Lineage I (**D**).

Table 4. Results of neutrality tests and mismatch distribution analysis for Clade 1, Clade 2, Lineage I, and the overall populations based on cpDNA.

Populations	τ	SSD (*p* Value)	HRag (*p* Value)	Tajima's D (*p* Value)	Fu's Fs (*p* Value)
Overall	4.379	0.034 (0.110)	0.064 (0.220)	1.956 (0.970)	5.793 (0.952)
Clade 1	4.326	0.043 (0.280)	0.136 (0.320)	1.119 (0.893)	4.028 (0.935)
Clade 2	2.742	0.183 (0.120)	0.736 (0.040)	2.322 (0.993)	4.467 (0.965)
Lineage I	0.703	0.026 (0.020)	0.204 (0.010)	0.105 (0.616)	1.296 (0.740)

HRag, Harpending's raggedness index; SSD, sum of squared deviations.

3.4. Phylogeny-Based Estimations of Divergence Times

The average divergence times of *S. centiflora* are shown in Figure 5. The initial divergence was estimated at approximately 1.2 Ma (95% HPD: 0.5–2.1 Mya) and the last divergence was estimated at approximately 0.2 Ma (95% HPD: 0–0.5 Mya) based on an assumed substitution rate of 1.52×10^{-9} s/s/y in cpDNA. Thus, the species divergence occurred in the Middle–Late Pleistocene.

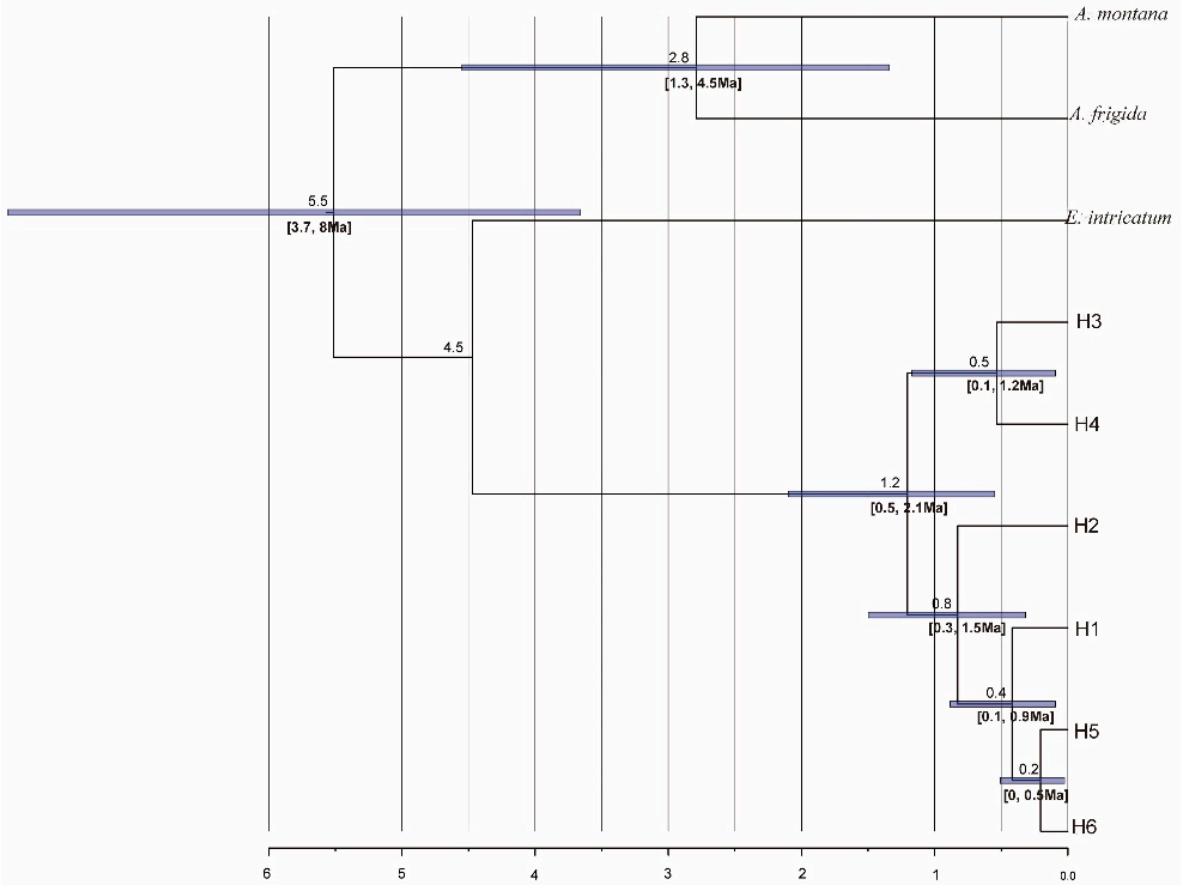

Figure 5. Bayesian divergence time estimates of *S. centiflora* based on the combined cpDNA data from two plastid gene markers (*trn*Q-*rps*16 and *psb*A-*trn*H). Blue bars on the nodes indicate 95% posterior credibility intervals.

4. Discussion

4.1. Genetic Diversity and Genetic Differentiation

Our results demonstrate that the 28 populations of *S. centiflora* have a high level of total haplotype diversity (H_T = 0.820) (Table 1). High cpDNA diversity has also been reported in several other endemic or relict species in Northwest China (*J. sabina* with H_T = 0.577 [14], *R. soongarica* with H_T = 0.607 [7], *G. przewalskii* with H_T = 0.849 [25], and *N. sphaerocarpa* with H_T = 0.887 [8]). A possible explanation for the high diversity in *S. centiflora* is its long evolutionary history, which may have allowed the accumulation of genetic variation. Moreover, the wide geographical range of this species across a geologically dynamic region provides ample opportunities for isolation, drift, and mutation.

A high level of cpDNA diversity was detected at the species level among populations (G_{ST} = 0.976); however, it was low (H_S = 0.020) within populations. Yet, the G_{ST} (0.976) of *S. centiflora* is higher than that of other angiosperm species (mean value of G_{ST} = 0.637 [59]). Low genetic diversity within populations and high genetic differentiation among populations indicate a lack of gene flow between populations for different reasons. Firstly, *S. centiflora* may have undergone long-term habitat fragmentation and geographic isolation among populations. This possibility has been interpreted as a consequence of strong bottlenecks or genetic drift associated with small effective population sizes for maternally inherited markers [60]. Secondly, high genetic differentiation among populations may also be due to limited gene flow through seeds associated either with geographical distance or mating system (either self-fertilization or clonal propagation, or both) [61]. This clearly applies for *S. centiflora*, which is hindered by geographic separation and physical barriers between deserts. In this manner, a high biologic heterogeneity may arise in desert land-

scapes. AMOVA revealed a marked differentiation between populations from different desert regions. Network and phylogenetic analyses also showed that ecological boundaries between the deserts limited gene flow in the species.

4.2. Identifying a Contact Zone between Deserts

Genetic divergence between lineages indicates a history of isolation. It is possible that the glacial cycling of the Plio-Pleistocene likely had a profound influence on the biogeographical history of species in this region. The continually shifting climates associated with Quaternary glacial oscillations would have dramatically affected diversification patterns within *S. centiflora*. During the Plio-Pleistocene, the climatic conditions in the deserts and steppes of Northwest China continuously varied. Steppes currently separate deserts; e.g., the Ordos grassland/steppe is located between the Kubuqi and Mu Us deserts. However, during the last glacial maximum of the Quaternary (approximately 18,000 years ago), the desert expansion in Northwest China would have also promoted desert species expansion [7]. Data regarding *S. centiflora* growing in different deserts provide strong evidence for the complex evolutionary history of this species.

Recent genetic research on the patterns of Quaternary contraction and expansion of many forest species in East China during glacial cycling has identified many refugia where multiple species survived the glacial maxima and contact zones where the same species from the different refugia met in the postglacial periods [62,63]. How can refugia and contact zones be distinguished? Generally, refugia have been identified by high levels of genetic diversity and private haplotypes within species. These haplotypes may not participate in the recolonization process and cannot be found elsewhere. Most importantly, haplotypes in refugia often have relatively close genetic relationships. However, haplotypes in the contact region genetically diverge. According to the phylogeny tree and haplotype network of cpDNA, the six chloroplast haplotypes found in our study can be divided into four lineages (I, II, III, IV) with high bootstrap supports (Figures 1A,B and 2). However, we could not detect any phylogeographic structure in N_{ST}/G_{ST} (Table 2), suggesting that the lineage admixture may exist. We found high genetic diversity, many haplotypes and ribotypes, and the occurrence of heterozygosity in the zones between the Tengger and Ulan Buh deserts. In addition, divergent haplotypes from Lineages III and IV are sympatrically distributed in these regions, suggesting that the region between the Tengger and Ulan Buh deserts is a contact zone into which different lineages dispersed from multiple refugia. Interestingly, Lineages II and III appear to be distributed strictly in an allopatric fashion; i.e., there was no contact zone between the two deserts. The most likely reason is that the impact of Quaternary climate change differed between the eastern (Kubuqi and Mu Us deserts) and western deserts (Badain Jaran, Tengger, and Ulan Buh deserts) [17]. The development and enlargement of mobile sand dunes were conducive to *S. centiflora* expansion, which resulted in haplotype sharing between the western deserts. However, the eastern deserts were less affected by Quaternary climate change than the western deserts. Therefore, semifixed or fixed sand dunes in the eastern deserts are not conducive to species expansion. Additional research must be conducted in the central Ordos area between the Kubuqi and Mu Us deserts to confirm this hypothesis and determine whether these two lineages come into contact.

4.3. nrDNA and cpDNA Variation

For *S. centiflora*, due to the arid desert environment, long distances between the five deserts, and consequent limitations on seed-mediated gene flow and pollinator movement, population discontinuities should be described by significant nrDNA and cpDNA variation. However, only cpDNA variation reflected significant genetic barriers. For the nrDNA ITS data, the AMOVA analysis showed that variation within populations was greater than that among populations (Table 3). The permutation test also revealed a significantly higher N_{ST} value than G_{ST} value in the ITS data but not in the cpDNA data (Table 2). The cpDNA data showed no shared haplotypes among the four groups or phylogeographical structure,

which likely occurred because of the discontinuous distribution of common haplotypes (e.g., H1 and H5) across different geographic regions; however, nrDNA had both. The inconsistency between the two datasets may be due to their different modes of inheritance and dispersal among populations (e.g., maternal vs. bipaternal, seeds vs. both seeds and pollen), faster substitution rates, and concerted evolution of nrITS sequences [64,65]. Therefore, nrDNA ribotypes represent gene flow by both seeds and pollen in *S. centiflora*, whereas the cpDNA haplotypes represent gene flow by seeds, which are more restricted among the four groups [58,66]. Our data suggest limited seed-mediated gene flow, but extensive pollen movement between desert ranges. From our result, we conclude that the ecological transition regions between deserts, as soft barriers, play distinct roles in limiting the gene flow when considering seed vs. pollen.

4.4. Relationship between Allopatric Divergence of S. centiflora and the Evolution of Deserts

Many studies had shown that the dramatic climate events of the Pleistocene era were critical to the formation and development of desert flora in Northwest China [7,8,25,67]. It is especially attractive to focus on the Pleistocene's glacial history and the formation of sandy habitats as key factors promoting adaptive divergence *S. centiflora*, which is endemic to sand dunes. Six cpDNA haplotypes were found in the 28 populations across the entire geographic distribution of *S. centiflora*. These haplotypes uniquely belonged to four distinct lineages in the phylogenetic tree (Figure 2), which is consistent with their respective distribution in four separate regions: Badain Jaran–Tengger, Ulan Buh, Kubuqi, and Mu Us deserts. Although this species shows allopatric distribution patterns, it is less geologically isolated. Interestingly, populations from four regions of *S. centiflora* in Northwest China showed significant genetic differentiation, especially at the cpDNA marker, with different chloroplast haplotypes fixed in each region. Similar allopatric divergence and fragmentation have been reported for *J. sabina* [14], *G. przewalskii* [25], and *N. sphaerocarpa* [8] in Northwest China.

We hypothesized that the five sand deserts in our study originated during the Quaternary period [16,17]. The sand deserts developed due to the mobilization of paleo-eolian sand, which likely occurred due to climate cooling and aridification driven by the marked Kun-Huang Movement (1.2, 0.8, 0.6 Ma) of QTP lift during the Quaternary [68], and climate oscillation during the Naynayxungla glacial period (1.2–0.6 Ma) [6,69,70]. Evidence from eolian sand, sediments, and fossil pollen indicate that the majority of the deserts' formation and expansion occurred at roughly 1.0 Ma [16,17]. Regarding the relationship between haplotype distribution and deserts, the history of desert development serves as a background and key to understanding the evolution of *S. centiflora*. Our molecular clock results (Figure 5) dated the separation of *S. centiflora* clades at 0.2~1.2 Ma during the Pleistocene. The timing entirely coincides with the known formation and development of the deserts, which implies that the evolution of *S. centiflora* may have been synchronous with their formation. The haplotypic genetic traits can be inferred to have originated in conjunction with the formation and development of the deserts since 1.8 Ma. In particular, starting from 1.2 Ma during the Quaternary, the Kun-Huang Movement of QTP lift and climate oscillation during the Naynayxungla glacial period were possible evolutionary driving forces. Geological and climate change events played important roles in sand desert formation in Northwest China because of lowered temperatures and increased aridity. Although Northwest China remained unglaciated, this period of intense climatic instability might have caused the fragmentation of species distributions, due to reductions in suitable habitats within the region, consequently leading to genetic differentiation among isolated region populations. In addition, gene flow among *S. centiflora* populations would have been readily interrupted due to its low seed dispersal capacity and the ecological barriers between deserts. Several animal and plant species have been studied that exhibited intraspecific diversifications that partly correspond with regional uplift and Quaternary glaciations of the Middle and Late Pleistocene [71–73].

5. Conclusions

The present phylogeographic study of *S. centiflora* based on cpDNA and ITS sequences reveals the influence of complex geological and climatic events on patterns of diversification and distribution in this endemic desert species. The major diversification of *S. centiflora* that occurred 1.2 Ma is likely related to geological movement and climate change. Furthermore, Pleistocene glacial cycles may have been important for structuring the four lineages found and creating the geographical contact zone between the WLBH and TGL deserts. Our results highlight a substantial contribution to our knowledge of past vegetation and climate dynamics in the arid land in Northwest China. However, further phylogeographic studies of *S. centiflora* are needed using whole genome sequence or genome-wide markers to address the conflicting results that we reported based on cpDNA and ITS sequences.

Supplementary Materials: The following supporting information can be downloaded at: https://www.mdpi.com/article/10.3390/d14020104/s1, Figure S1: Map of sites for the species *Stilpnolepis centiflora* in the arid lands of Northwest China. Location details are given in Table 1 and the reference [37], Figure S2: Correlation between the F statistics and grouping number (K = 2–14) from the SAMOVA results based on cpDNA, Figure S3: Inference of K, the most probable number of clusters, and the proportion of genetic clusters, using Structure software. Analysis was performed based on cpDNA analysis of 280 samples of *Stilpnolepis centiflora*. (a) Proportion of genetic clusters at K = 2 and K = 4 for each of the 280 *Stilpnolepis centiflora* individuals. The smallest vertical bar represents one individual. The assignment proportion of each individual into population clusters is shown along the *y*-axis. (b) The first analysis was conducted based on cpDNA analysis of 280 samples of *Stilpnolepis centiflora*, at K = 2; the log-likelihood value of the data (Delta K) as a function of K was calculated over ten replicates. (c) The second analysis was conducted excluding populations from the TGL-BDJL group, at K = 3; the log-likelihood value of the data (Delta K) as a function of K was calculated over ten replicates. Figure S4: Scatterplots representing relationships between genetic distance and geographic distance of the species based on cpDNA (A) and nrDNA (B), Figure S5: Phylogenetic NJ-tree of ribotypes, Table S1: Summary of 28 populations used in the present study, including voucher information, Table S2: The haplotype sequences of the two chloroplast DNA fragments of 280 individuals from 28 populations of *S. centiflora* from five deserts in Northwest China used in analysis with corresponding GenBank reference numbers for each haplotype, Table S3: The ribotype sequences based on the ITS fragment from 250 individuals of *S. centiflora* from five deserts in Northwest China used in analysis with corresponding GenBank reference numbers for each ribotype, Table S4: Summary of the six haplotypes (H1–H6) based on aligned sequences of the two chloroplast DNA fragments of 280 individuals and 28 populations of *S. centiflora* from five deserts in Northwest China, Table S5: Summary of the 31 ribotypes (R1–R31) based on aligned sequences of ITS fragments from 250 individuals and 28 populations of *S. centiflora* sampled from five deserts in Northwest China.

Author Contributions: Conceptualization, X.S.; methodology, X.S., X.J. and H.Z.; investigation, data curation, X.S., X.J. and J.Q.; formal analysis, X.S. and X.J.; resources, X.S., X.J., H.Z. and J.Q.; writing—original draft preparation, X.S.; writing—review and editing, X.S., X.J., H.Z. and J.Q. All authors have read and agreed to the published version of the manuscript.

Funding: This research was financially supported by the National Natural Science Foundation of China (31960229, 31760139, 31760060) and Excellent Youth Foundation of Natural Science Foundation of Xinjiang Uygur Autonomous Region of China (2021D01E21).

Institutional Review Board Statement: Not applicable.

Data Availability Statement: Sequences are available on GenBank (see Supplementary Tables S2 and S3).

Acknowledgments: We are grateful to Carol C. Baskin, Jerry M. Baskin, Stewart C. Sanderson and the anonymous referee for their helpful comments and careful English correction.

Conflicts of Interest: The authors declare no competing interests.

References

1. Manel, S.; Holderegger, R. Ten years of landscape genetics. *Trends Ecol. Evol.* **2013**, *28*, 614–621. [CrossRef] [PubMed]
2. Avise, J. *Phylogeography: The History and Formation of Species*; Harvard University Press: Cambridge, MA, USA, 2000.
3. Hewitt, G.M. The genetic legacy of the Quaternary ice ages. *Nature* **2000**, *405*, 907–913. [CrossRef] [PubMed]
4. Hewitt, G.M. Genetic consequences of climatic oscillations in the Quaternary. *Philos. Trans. R. Soc. B Biol. Sci.* **2004**, *359*, 183–195. [CrossRef]
5. Wang, S.M.; Zhang, X.; Li, Y.; Zhang, L.; Xiong, Y.C.; Wang, G. Spatial distribution patterns of the soil seed bank of *Stipagrostis pennata* (Trin.) de Winter in the Gurbantonggut Desert of north-west China. *J. Arid. Environ.* **2005**, *63*, 203–222. [CrossRef]
6. Zheng, B.; Xu, Q.; Shen, Y. The relationship between climate change and Quaternary glacial cycles on the Qinghai–Tibetan Plateau: Review and speculation. *Quat. Int.* **2002**, *97–98*, 93–101. [CrossRef]
7. Li, Z.-H.; Chen, J.; Zhao, G.-F.; Guo, Y.-P.; Kou, Y.-X.; Ma, Y.-Z.; Wang, G.; Ma, X.-F. Response of a desert shrub to past geological and climatic change: A phylogeographic study of *Reaumuria soongarica* (Tamaricaceae) in western China. *J. Syst. Evol.* **2012**, *50*, 351–361. [CrossRef]
8. Su, Z.; Zhang, M. Evolutionary response to Quaternary climate aridification and oscillations in north-western China revealed by chloroplast phylogeography of the desert shrub *Nitraria sphaerocarpa* (Nitrariaceae). *Biol. J. Linn. Soc.* **2013**, *109*, 757–770. [CrossRef]
9. Riddle, B.R.; Honeycutt, R.L. Historical biogeography in North-American arid regions—An approach using mitochondrial-dna phylogeny in grasshopper mice (genus *Onychomys*). *Evolution* **1990**, *44*, 1–15.
10. Riddle, B.R.; Hafner, D.J.; Alexander, L.F. Comparative Phylogeography of Baileys' Pocket Mouse (Chaetodipus baileyi) and the Peromyscus eremicus Species Group: Historical Vicariance of the Baja California Peninsular Desert. *Mol. Phylogenetics Evol.* **2000**, *17*, 161–172. [CrossRef]
11. Riddle, B.R.; Hafner, D.J.; Alexander, L.F. Phylogeography and Systematics of the Peromyscus eremicus Species Group and the Historical Biogeography of North American Warm Regional Deserts. *Mol. Phylogenetics Evol.* **2000**, *17*, 145–160. [CrossRef]
12. Leache, A.D.; Mulcahy, D.G. Phylogeny, divergence times and species limits of spiny lizards (Sceloporus magister species group) in western North American deserts and Baja California. *Mol. Ecol.* **2007**, *16*, 5216–5233. [CrossRef]
13. Jaeger, J.R.; Riddle, B.R.; Bradford, D.F. Cryptic Neogene vicariance and Quaternary dispersal of the red-spotted toad (*Bufo punctatus*): Insights on the evolution of North American warm desert biotas. *Mol. Ecol.* **2005**, *14*, 3033–3048. [CrossRef]
14. Guo, Y.-P.; Zhang, R.; Chen, C.-Y.; Zhou, D.-W.; Liu, J.-Q. Allopatric divergence and regional range expansion of *Juniperus sabina* in China. *J. Syst. Evol.* **2010**, *48*, 153–160. [CrossRef]
15. Dong, G.R.; Li, B.S.; Gao, S.Y.; Wu, Z.; Shao, Y.J. Discovery of Quaternary ancient eolian sands and its significance in the Ordos Plateau. *Chin. Sci. Bull.* **1983**, *4*, 998–1001.
16. Dong, G.R.; Chen, H.Z.; Jin, J.; Wang, G.Y. Resent advancing on Quaternary research in desert area, North China. *Prog. Geo.* **1991**, *6*, 29–32.
17. Dong, G.; Li, S.; Li, B.S.; Wang, Y.; Yan, M.C. A preliminary study on the formation and evolution of deserts in China. *J. Desert Res.* **1991**, *11*, 23–32.
18. Wang, Y.; Li, S.; Wang, J.H.; Yan, M.C. The uplift of the Qinghai-Xizang (Tibetan) Plateau and its effect on the formation and evolution of Chinese deserts. *Arid Zone Res.* **1996**, *13*, 20–24.
19. Zheng, H.B.; Powell, C.M.; Butcher, K.; Cao, J.J. Late Neogene loess deposition in southern Tarim Basin: Tectonic and palaeo-environmental implications. *Tectonophysics* **2003**, *375*, 49–59. [CrossRef]
20. Sun, J.; Zhang, L.; Deng, C.; Zhu, R. Evidence for enhanced aridity in the Tarim Basin of China since 5.3Ma. *Quat. Sci. Rev.* **2008**, *27*, 1012–1023. [CrossRef]
21. Fang, X.; Lü, L.; Yang, S.; Li, J.; An, Z.; Jiang, P.; Chen, X. Loess in Kunlun Mountains and its implications on desert development and Tibetan Plateau uplift in west China. *Sci. China Ser. D Earth Sci.* **2002**, *45*, 289–299. [CrossRef]
22. Sun, J. Source Regions and Formation of the Loess Sediments on the High Mountain Regions of Northwestern China. *Quat. Res.* **2002**, *58*, 341–351. [CrossRef]
23. Yang, X.; Rost, K.T.; Lehmkuhl, F.; Zhenda, Z.; Dodson, J. The evolution of dry lands in northern China and in the Republic of Mongolia since the Last Glacial Maximum. *Quat. Int.* **2004**, *118–119*, 69–85. [CrossRef]
24. Hoskin, C.J.; Higgie, M.; McDonald, K.R.; Moritz, C. Reinforcement drives rapid allopatric speciation. *Nature* **2005**, *437*, 1353–1356. [CrossRef]
25. Ma, S.; Zhang, M. Phylogeography and conservation genetics of the relic *Gymnocarpos przewalskii* (Caryophyllaceae) restricted to northwestern China. *Conserv. Genet.* **2012**, *13*, 1531–1541. [CrossRef]
26. Shi, Z.; Humphries, C.J.; Gilbert, M.G. Asteraceae (Compositae). In *Flora of China*; Wu, Z.Y., Raven, P.H., Eds.; Science Press: Beijing, China; Missouri Botanical Garden Press: St. Louis, MO, USA, 2011; Volume 20–21, pp. 758–759.
27. Zhao, Y.Z. The area and floristic grographic element of *Stilpnolepis centiflora*. *J. Inn. Mong. Univ.* **1996**, *27*, 662–663.
28. Pellicer, J.; Hidalgo, O.; Garcia, S.; Garnatje, T.; Korobkov, A.A.; Valles, J.; Martin, J. Palynological study of Ajania and related genera (Asteraceae, Anthemideae). *Bot. J. Linn. Soc.* **2009**, *161*, 171–189. [CrossRef]
29. Liu, Y.; Yang, S.-X.; Ji, P.-Z.; Gao, L.-Z. Phylogeography of *Camellia taliensis* (Theaceae) inferred from chloroplast and nuclear DNA: Insights into evolutionary history and conservation. *BMC Evol. Biol.* **2012**, *12*, 92. [CrossRef]

30. Turchetto-Zolet, A.C.; Cruz, F.; Vendramin, G.G.; Simon, M.F.; Salgueiro, F.; Margis-Pinheiro, M.; Margis, R. Large-scale phylogeography of the disjunct Neotropical tree species *Schizolobium parahyba* (Fabaceae-Caesalpinioideae). *Mol. Phylogenet Evol.* **2012**, *65*, 174–182. [CrossRef]
31. Cullings, K. Design and testing of a plant-specific PCR primer for ecological and evolutionary studies. *Mol. Ecol.* **1992**, *1*, 233–240. [CrossRef]
32. Shaw, J.; Lickey, E.B.; Beck, J.T.; Farmer, S.B.; Liu, W.; Miller, J.; Siripun, K.C.; Winder, C.T.; Schilling, E.E.; Small, R.L. The tortoise and the hare II: Relative utility of 21 noncoding chloroplast DNA sequences for phylogenetic analysis. *Am. J. Bot.* **2005**, *92*, 142–166. [CrossRef]
33. Shaw, J.; Lickey, E.B.; Schilling, E.E.; Small, R.L. Comparison of whole chloroplast genome sequences to choose noncoding regions for phylogenetic studies in angiosperms: The tortoise and the hare III. *Am. J. Bot.* **2007**, *94*, 275–288. [CrossRef] [PubMed]
34. White, T.J.; Burns, T.; Lee, S.; Taylor, J. *Amplification and Direct Sequencing of Fungal Ribosomal RNA Genes for Phylogenetics*; Academic Press: New York, NY, USA, 1990.
35. Thompson, J.D.; Gibson, T.J.; Plewniak, F.; Jeanmougin, F.; Higgins, D.G. The CLUSTAL_X windows interface: Flexible strategies for multiple sequence alignment aided by quality analysis tools. *Nucleic Acids Res.* **1997**, *25*, 4876–4882. [CrossRef] [PubMed]
36. Librado, P.; Rozas, J. DnaSP v5: A software for comprehensive analysis of DNA polymorphism data. *Bioinformatics* **2009**, *25*, 1451–1452. [CrossRef] [PubMed]
37. Garrick, R.C.; Sunnucks, P.; Dyer, R.J. Nuclear gene phylogeography using PHASE: Dealing with unresolved genotypes, lost alleles, and systematic bias in parameter estimation. *BMC Evol. Biol.* **2010**, *10*, 118. [CrossRef]
38. Tamura, K.; Stecher, G.; Kumar, S. MEGA11: Molecular Evolutionary Genetics Analysis Version 11. *Mol. Biol. Evol.* **2021**, *38*, 3022–3027. [CrossRef]
39. Kimura, M. A simple method for estimating evolutionary rates of base substitutions through comparative studies of nucleotide sequences. *J. Mol. Evol.* **1980**, *16*, 111–120. [CrossRef]
40. Bandelt, H.J.; Forster, P.; Rohl, A. Median-joining networks for inferring intraspecific phylogenies. *Mol. Biol. Evol.* **1999**, *16*, 37–48. [CrossRef]
41. Cassens, I.; Mardulyn, P.; Milinkovitch, M.C. Evaluating intraspecific "Network" construction methods using simulated se-quence data: Do existing algorithms outperform the global maximum parsimony approach? *Syst. Biol.* **2005**, *54*, 363–372. [CrossRef]
42. Excoffier, L.; Lischer, H.E.L. Arlequin suite ver 3.5: A new series of programs to perform population genetics analyses under Linux and Windows. *Mol. Ecol. Resour.* **2010**, *10*, 564–567. [CrossRef]
43. Miller, M.P. Alleles In Space (AIS): Computer software for the joint analysis of interindividual spatial and genetic information. *J. Hered.* **2005**, *96*, 722–724. [CrossRef]
44. Pons, O.; Petit, R.J. Measuring and Testing Genetic Differentiation with Ordered versus Unordered Alleles. *Genetics* **1996**, *144*, 1237–1245. [CrossRef]
45. Dupanloup, I.; Schneider, S.; Excoffier, L. A simulated annealing approach to define the genetic structure of populations. *Mol. Ecol.* **2002**, *11*, 2571–2581. [CrossRef]
46. Evanno, G.; Regnaut, S.; Goudet, J. Detecting the number of clusters of individuals using the software STRUCTURE: A simulation study. *Mol. Ecol.* **2005**, *14*, 2611–2620. [CrossRef]
47. Pritchard, J.K.; Stephens, M.; Donnelly, P. Inference of population structure using multilocus genotype data. *Genetics* **2000**, *155*, 945–959. [CrossRef]
48. Earl, D.A.; Vonholdt, B.M. Structure Harvester: A website and program for visualizing STRUCTURE output and implementing the Evanno method. *Conserv. Genet. Resour.* **2012**, *4*, 359–361. [CrossRef]
49. Excoffier, L.; Smouse, P.E.; Quattro, J.M. Analysis of Molecular Variance Inferred from Metric Distances among DNA Haplotypes—Application to Human Mitochondrial-DNA Restriction Data. *Genetics* **1992**, *131*, 479–491. [CrossRef]
50. Drummond, A.J.; Rambaut, A. BEAST: Bayesian evolutionary analysis by sampling trees. *BMC Evol. Biol.* **2007**, *7*, 1–8. [CrossRef]
51. Wang, J.-F.; Gong, X.; Chiang, Y.-C.; Kuroda, C. Phylogenetic patterns and disjunct distribution in *Ligularia hodgsonii* Hook. (Asteraceae). *J. Biogeogr.* **2013**, *40*, 1741–1754. [CrossRef]
52. Rambaut, A.; Drummond, A.J. Tracer v. 1.5. 2009. Available online: http://tree.bio.ed.ac.uk/software/tracer/ (accessed on 25 March 2014).
53. Rambaut, A. FigTree v. 1.3.1. 2009. Available online: http://tree.bio.ed.ac.uk/software/FigTree/ (accessed on 5 May 2012).
54. Tajima, F. Statistical method for testing the neutral mutation hypothesis by DNA polymorphism. *Genetics* **1989**, *123*, 585–595. [CrossRef]
55. Fu, Y.-X. Statistical Tests of Neutrality of Mutations Against Population Growth, Hitchhiking and Background Selection. *Genetics* **1997**, *147*, 915–925. [CrossRef]
56. Slatkin, M.; Hudson, R.R. Pairwise comparisons of mitochondrial DNA sequences in stable and exponentially growing populations. *Genetics* **1991**, *129*, 555–562. [CrossRef]
57. Schneider, S.; Excoffier, L. Estimation of past demographic parameters from the distribution of pairwise differences when the mutation rates very among sites: Application to human mitochondrial DNA. *Genetics* **1999**, *152*, 1079–1089. [CrossRef]
58. Wolfe, K.H.; Li, W.-H.; Sharp, P.M. Rates of nucleotide substitution vary greatly among plant mitochondrial, chloroplast, and nuclear DNAs. *Proc. Natl. Acad. Sci. USA* **1987**, *84*, 9054–9058. [CrossRef]

59. Petit, R.J.; Duminil, J.; Fineschi, S.; Hampe, A.; Salvini, D.; Vendramin, G.G. Comparative organization of chloroplast, mitochondrial and nuclear diversity in plant populations. *Mol. Ecol.* **2005**, *14*, 689–701. [CrossRef]
60. Birky, C.W., Jr.; Fuerst, P.; Maruyama, T. Organelle gene diversity under migration, mutation, and drift: Equilibrium expectations, approach to equilibrium, effects of heteroplasmic cells, and comparison to nuclear genes. *Genetics* **1989**, *121*, 613–627. [CrossRef]
61. Petit, R.J.; Aguinagalde, I.; de Beaulieu, J.-L.; Bittkau, C.; Brewer, S.; Cheddadi, R.; Ennos, R.; Fineschi, S.; Grivet, D.; Lascoux, M.; et al. Glacial Refugia: Hotspots but Not Melting Pots of Genetic Diversity. *Science* **2003**, *300*, 1563–1565. [CrossRef]
62. Qiu, Y.-X.; Fu, C.-X.; Comes, H.P. Plant molecular phylogeography in China and adjacent regions: Tracing the genetic imprints of Quaternary climate and environmental change in the world's most diverse temperate flora. *Mol. Phylogenetics Evol.* **2011**, *59*, 225–244. [CrossRef]
63. Liu, J.Q.; Sun, Y.S.; Ge, X.J.; Gao, L.M.; Qiu, Y.X. Phylogeographic studies of plants in China: Advances in the past and directions in the future. *J. Syst. Evol.* **2012**, *50*, 267–275. [CrossRef]
64. Alvarez, I.; Wendel, J.F. Ribosomal ITS sequences and plant phylogenetic inference. *Mol. Phylogenet Evol.* **2003**, *29*, 417–434. [CrossRef]
65. Lorenz-Lemke, A.P.; Muschner, V.C.; Bonatto, S.L.; Cervi, A.C.; Salzano, F.M.; Freitas, L.B. Phylogeographic inferences concerning evolution of Brazilian *Passiflora actinia* and *P. elegans* (Passifloraceae) based on ITS (nrDNA) variation. *Ann. Bot.* **2005**, *95*, 799–806. [CrossRef] [PubMed]
66. Schaal, B.A.; Hayworth, D.A.; Olsen, K.M.; Rauscher, J.T.; Smith, W.A. Phylogeographic studies in plants: Problems and pro-spects. *Mol. Ecol.* **1998**, *7*, 465–474. [CrossRef]
67. Meng, H.-H.; Zhang, M.-L. Diversification of plant species in arid Northwest China: Species-level phylogeographical history of Lagochilus Bunge ex Bentham (Lamiaceae). *Mol. Phylogenetics Evol.* **2013**, *68*, 398–409. [CrossRef] [PubMed]
68. Li, J.J.; Shi, Y.F.; Li, B.Y. *Uplift of the Qinghai-Xizang (Tibet) Plateau and Global Change Lanzhou*; Lanzhou University Press: Lanzhou, China, 1995.
69. Shi, Y.F.; Zheng, B.X.; Li, S.J. Last glaciation and maximum glaciation in Qinghai-Xizang (Tibet) plateau. *J. Glaciol. Geocryol.* **1990**, *12*, 1–15.
70. Zhou, S.; Li, J. The sequence of Quaternary glaciation in the Bayan Har Mountains. *Quat. Int.* **1998**, *45–46*, 135–142. [CrossRef]
71. Yang, S.-J.; Yin, Z.-H.; Ma, X.-M.; Lei, F.-M. Phylogeography of ground tit (*Pseudopodoces humilis*) based on mtDNA: Evidence of past fragmentation on the Tibetan Plateau. *Mol. Phylogenetics Evol.* **2006**, *41*, 257–265. [CrossRef]
72. Qi, D.; Guo, S.; Zhao, X.; Yang, J.; Tang, W. Genetic diversity and historical population structure of *Schizopygopsis pylzovi* (Teleostei: Cyprinidae) in the Qinghai?Tibetan Plateau. *Freshw. Biol.* **2007**, *52*, 1090–1104. [CrossRef]
73. Jin, Y.T.; Brown, R.P.; Liu, N.F. Cladogenesis and phylogeography of the lizard *Phrynocephalus vlangalii* (Agamidae) on the Tibetan plateau (vol 17, pg 1971, 2008). *Mol. Ecol.* **2008**, *17*, 3033–3034.